Journal of Pharmaceutical Analysis 8 (2018) 258–264

Contents lists available at ScienceDirect

Journal of Pharmaceutical Analysis

journal homepage: www.elsevier.com/locate/jpa
www.sciencedirect.com

Original Research Article

Extracellular synthesis of silver nanoparticles by *Pseudomonas* sp. THG-LS1.4 and their antimicrobial application

Hina Singh [a], Juan Du [a,b], Priyanka Singh [a], Tae Hoo Yi [a,*]

[a] Department of Oriental Medicine Biotechnology, College of Life Science, Kyung Hee University Global Campus, 1732 Deokyoungdaero, Giheung-gu, Yongin-si, Gyeonggi-do 446-701, Republic of Korea
[b] College of Food and Bioengineering, Zhengzhou University of Light Industry, Henan Province Collaborative Innovation Center for Food Production and Safety, Zhengzhou 450001, China

ARTICLE INFO

Article history:
Received 18 September 2017
Received in revised form
15 January 2018
Accepted 19 April 2018
Available online 20 April 2018

Keywords:
Extracellular synthesis
Silver nanoparticles
Pseudomonas sp. THG-LS1.4
Antimicrobial activity

ABSTRACT

Silver nanoparticles (AgNPs) are known to have bacteriostatic and bactericidal effects. The present study highlights the extracellular synthesis of AgNPs and its antibacterial properties. The AgNPs were synthesized using *Pseudomonas* sp. THG-LS1.4 strain which had been isolated from soil. The AgNPs were characterized by field emission-transmission electron microscopy (FE-TEM), X-ray diffraction (XRD), Fourier transform-infrared (FT-IR) spectroscopy, and particle size distribution (DLS). The AgNPs displayed maximum absorbance at 412 nm and were irregular in shape ranging from 10 to 40 nm. The XRD spectroscopy results demonstrated the crystalline nature of nanoparticles. The AgNPs showed antimicrobial activity against *Bacillus cereus*, *Staphylococcus aureus*, *Candida tropicalis*, *Vibrio parahaemolyticus*, *Escherichia coli* and *Pseudomonas aeruginosa*. Furthermore, the AgNPs were also evaluated for their increased antibacterial activities with various antibiotics against *Escherichia coli*, *Pseudomonas aeruginosa* and *Salmonella enterica*. Additionally, AgNPs showd biofilm inhibition activity. The biosynthesized AgNPs were found to be a potent agent against tested pathogens. More importantly, we highlight the applications of AgNPs as an antimicrobial agent.

1. Introduction

Nanotechnology is emerging as a rapidly growing field with its application in science and technology for the purpose of manufacturing new materials at the nanoscale level [1]. Bionanotechnology has emerged as integration between biotechnology and nanotechnology for developing biosynthetic and eco-friendly technology for synthesis of nanomaterials and nanoparticles. Various types of nanoparticles have been reported like copper, zinc, titanium, magnesium, gold, alginate and silver [2–5]. However, silver nanoparticles (AgNPs) have potential applications in the fields of medical nano-engineering and pharmaceutical for the development of therapeutic agents, chronic disease diagnostics and biosensors [6]. AgNPs are known to have antimicrobial efficacy against bacteria, viruses and eukaryotic micro-organisms [7,8]. Because of its antibacterial properties, AgNPs are incorporated in apparel, footwear, paints, wound dressings, appliances, cosmetics, and plastics. The exact mechanism behind antibacterial efficacy of AgNPs is still not clear, but there are various proposed mechanisms of action for nanoparticles, including disturbance of the cell membrane; alteration of cellular DNA and proteins, electron transport, nutrient uptake, protein oxidation, or membrane potential; or the generation of ROS, which lead to cell death [9]. Silver at the nanostructure level has gained considerable attention due to its antimicrobial, anticoagulant, biofilm inhibition, anticancer and anti-inflammatory efficacies which make it an ideal candidate in medical and biological platform [10].

The chemical and physical methods used for the synthesis of nanoparticles make a large amount of hazardous byproducts and hence are the major concern for environmental contamination [11]. Most of the techniques are expensive, as well as inefficient in materials and energy use. Hence, there is an ever-growing need to develop clean, nontoxic, and environmentally benign synthetic procedures. Consequently, researchers have used biological synthesis. The main reason for this may be that the processes devised by nature for the synthesis of inorganic materials on nano- and micro-scales have contributed to the development of a relatively new and largely unexplored area of research based on the use of microbes in the biosynthesis of nanomaterials [12]. Among the microorganisms, bacteria have received the most attention in

Peer review under responsibility of Xi'an Jiaotong University.
* Corresponding author.
E-mail address: drhoo@khu.ac.kr (T.H. Yi).

https://doi.org/10.1016/j.jpha.2018.04.004

bio-synthesis of nanoparticles due to its growing success, ease of handling and genetic modification [13]. Recently several microorganisms, such as *Bhargavaea indica*, *Pseudomonas deceptionensis,* and *Bacillus methylotrophicus,* have been isolated for extracellular synthesis of anisotropic and spherical AgNPs, respectively [8,14,15]. The aforementioned strains have been reported from soil. Here, *Psuedomonas* sp. THG-LS1.4 strain isolated from soil has been employed for the synthesis of AgNPs.

The approach on using culture supernatants from different bacteria for the synthesis of AgNPs is well known. Culture supernatant contains reductases, produced and secreted by microorganisms [16,17], which is responsible for production of nanoparticles. In the present study, we used the culture supernatant for the green synthesis of AgNPs without the addition of a reducing agent. The synthesized AgNPs were further characterized and also evaluated for the antimicrobial activity against pathogenic microorganisms. The adopted method for synthesis is simple, straightforward, and convenient. Further, this is for the first time that *Pseudomonas* sp. THG-LS1.4 has been reported for the synthesis of AgNPs.

2. Experimental

2.1. Materials

Media and antibiotics were purchased from Oxoid Ltd., England. All the chemicals were purchased from Sigma-Aldrich Chemicals, USA. The pathogenic bacterial strains were obtained from Korean Agricultural Culture Collection (KACC) and Korean Collection for Type Cultures (KCTC).

2.2. Bacterial isolation and molecular characterization

The bacterial strain THG-LS1.4 was isolated from soil sample collected from Kyung Hee University, South Korea. The soil sample was serially diluted in sterile 0.85% NaCl and then spread onto nutrient agar (NA) containing Lab-Lemco powder 1.0 g, yeast extract 1.0 g, peptone 5.0 g, sodium chloride 5.0 g, and agar 15.0 g in 1000 mL distill water pH 7.0, to obtain isolated colonies. The isolated colonies were further cultured on NA plate supplemented with 1 mM silver nitrate ($AgNO_3$) followed by incubation at 28 °C for 48 h. After incubation period the bacterial growth was checked.

Genomic DNA of strain THG-LS1.4 was extracted and purified using a commercial Genomic DNA extraction kit (Solgent, Korea). The 16S rRNA gene was amplified with the universal bacterial primer pair 27F and 1492R and the purified PCR products were sequenced by Solgent Co., Ltd (Daejeon, Korea). The 16S rRNA gene sequences of related taxa were obtained from the EzTaxon-e server and GenBank database [18]. Phylogenetic tree was constructed with neighbor joining method [19] by using the MEGA 6 program package [20] to demonstrate the phylogenetic position of the isolated strain. The strain was maintained on NA medium and stored as suspension in nutrient broth (NB) with glycerol 25% (v/v) at −80 °C.

Enzyme activities and other biochemical characteristics were tested by using API 20 NE and API ZYM kits according to the instructions of the manufacturer (bioMe´rieux, France). API 20 NE strips were read after 24 and 48 h, and API ZYM strips were checked after 12 h of incubation at 28 °C.

2.3. Extracellular synthesis of AgNPs

Pseudomonas sp. THG-LS1.4 was cultured in 100 mL of NB medium. The flask was incubated for one day at 28 °C in an orbital shaker (120 rpm) and then the medium was centrifuged to obtain supernatant. The supernatant was mixed with filter sterilized $AgNO_3$ solution at 1 mM final concentration, and further incubated at 120 rpm and 28 °C for 48 h. The synthesis was monitored for a change in the color of the culture medium by visual inspection. The AgNPs were collected by high speed centrifugation at 12,000 *g* and 25 °C for 10 min (Beckman Coulter, Avanti™ J-25 centrifuge, USA) and washed thoroughly by water to remove the unconverted metal ions or any other constituents. The purified nanoparticles were air dried and obtained in powder form.

2.4. Characterization of AgNPs

2.4.1. UV–visible spectrophotometer (UV–vis)

The bio-reduction of Ag^+ ions was monitored with UV–visible spectra and recorded with UV–vis spectrophotometer (Optizen POP; Mecasys) from 300 to 800 nm.

2.4.2. Field emission-transmission electron microscopy (FE-TEM)

The morphology, purity and elemental compositions of synthesized AgNPs were examined using FE-TEM, energy dispersive X-ray (EDX) spectroscopy, elemental mapping and selected area diffraction pattern (SAED) with a TEM-2100F (JEOL) electron microscope operated at 200 kV. The sample for FE-TEM was prepared by placing a drop of AgNPs solution on carbon coated copper grid, drying at room temperature and transferring it to the microscope.

2.4.3. X-ray diffraction (XRD)

The XRD analyses were performed on X-ray diffractometer (D8 Advance, Bruker, Germany), operated at 40 kv, 40 mA, with CuKα radiation, at a scanning rate of 6°/min, step size of 0.02, over the 2θ range of 20–80°. For XRD the samples were freeze dried and obtained in powdered form. For freeze drying the AgNPs collected after centrifuge were kept at −80 °C for 2 h and then put to freeze dryer (Ilshin lab Co. Ltd, South Korea).

2.4.4. Fourier transform-infrared (FT-IR) spectroscopy

The FT-IR spectral studies establish the biomolecules which are responsible for stabilization and capping of AgNPs. The spectrum was recorded on Perkin Elmer Fourier transform infrared spectrometer in the range of 400–4000 cm^{-1} with a resolution of 4 cm^{-1}. For FT-IR the samples were freeze dried and obtained in powdered form.

2.4.5. Particle size distribution (DLS)

Particle size of AgNP was measured in triplicate using Zetasizer Nano ZS90 (Malvern Instruments, UK) at 25 °C and at a 12 angle. Pure water with a refractive index of 1.3328, viscosity of 0.8878 cP, and dielectric constant of 78.3 was used as a dispersive medium.

2.5. Antimicrobial activity of AgNPs

2.5.1. Disc diffusion assay

Disc diffusion method was followed to analyze the antimicrobial activity of AgNPs. All the pathogenic microbes were grown overnight in Mueller-Hinton broth (MHB). 100 µL culture of each strain was spread evenly on a Mueller-Hinton agar (MHA) plate. Paper discs (8 mm) containing 30 µL of the AgNPs (500 ppm in water) was placed over the MHA plates. The plates were incubated at 28 °C for 24 h.

Similarly, the antibacterial effect in combination with commercial antibiotics like erythromycin (15 µg/disc), novobiocin (30 µg/disc), lincomycin (15 µg/disc), penicillin G (10 µg/disc), vancomycin (30 µg/disc) and oleandomycin (15 µg/disc) has been tested against *P. aeruginosa*, *E. coli* and *S. enterica*. Antibiotics discs without AgNPs were treated as control. After 24 h, the zones of inhibition were measured. The study was done in triplets.

2.5.2. Biofilm inhibition assay

The biofilm degrading activity of AgNPs was determined by colorimetric method against *S. aureus* and *P. aeruginosa*. Culture of *S. aureus* and *P. aeruginosa* grown in NB (optical density of 0.1 at 620 nm) having cell count of 108 cfu/mL was used. The culture (190 µL) was dispensed in 96 wells of sterile polystyrene microtiter plate. After culturing for 24 h, 10 µL different concentrations of AgNPs ranging from 2 to 10 µg/mL were added.

Wells with 200 µL culture and no AgNPs were kept as a control. Samples were withdrawn after 24 h and crystal violet biofilm (CVB) assay was performed [14]. The absorbance of each well was measured at 595 nm using a microtiter ELISA reader (Molecular Devices E09090). The experiments were performed in triplets and results were interpreted in terms of mean with ± standard deviation.

3. Results and discussion

3.1. Molecular characterization of AgNPs producing strain

The 16S rRNA gene sequence of strain THG-LS1.4 was a continuous stretch of 1454 bp and the sequence has been submitted to NCBI (NCBI GenBank accession number KU523693). Sequence similarity calculation using the EzTaxon-e server indicated that the strain shares highest sequence similarity (99.7%) with *Psuedomonas koreensis*. The phylogenetic trees also indicated that strain THG-LS1.4 was affiliated with the genus *Psuedomonas* and formed a phyletic line distinct from the clades of related species (Fig. 1). Results of biochemical characteristics performed using API 20 NE and API ZYM are represented in Table 1.

3.2. Extracellular synthesis of AgNPs

Firstly, the extracellular synthesis of nanoparticles was confirmed by visual observation with the appearance of color change in the reaction mixture. The color of supernatant changed from yellow to deep brown within 48 h, the color intensity increased with period of incubation due to the reduction in Ag^0. Control (without bacteria) showed no color change when incubated for the same period and condition. The change in color from pale yellow to dark brown was attributed to surface plasmon resonance. Similar observation was made by Singh et al.[10] in the extracellular synthesis of AgNPs by *Sporosarcina koreensis* DC4 strain by extracellular process.

There are two types of synthesis methods which can be classified as intracellular and extracellular depending on the location of nanoparticles formed. The exact mechanism for the synthesis of AgNPs by bacteria was not fully understood. However, reports

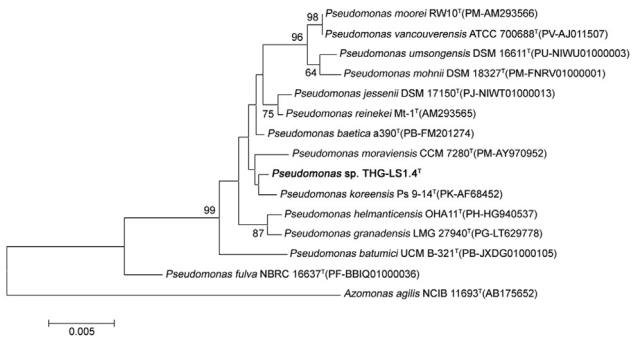

Fig. 1. Neighbor-joining phylogenetic tree based on 16S rRNA gene sequences showing the relationships of strain THG-LS1.4 with related species. Bootstrap values (expressed as percentage of 1000 replications) are shown at branch points. Bar, 0.005 substitutions per nucleotide position.

Table 1
Biochemical tests result of *Pseudomonas koreensis* THG-LS1.4.

API 20 NE	Result	API ZYM (enzymatic activity)	Result
Nitrate reduction	–	Alkaline phosphatase	+
Indole production	–	Esterase (C4)	+
Glucose Acidification	–	Esterase Lipase (C8)	+
Arginine dihydrolase	+	Lipase (C14)	–
Urease	+	Leucine arylamidase	+
Esculin hydrolysis	–	Valine arylamidase	w
Protease (gelatin hydrolysis)	+	Cystine arylamidase	–
β-Galactosidase (PNPG)	–	Trypsin	–
D-Glucose	+	α-Chymotrypsin	–
L-Arabinose	+	Acid phosphatase	+
D-Mannose	+	Naphtol-*AS-BI*-phosphohydrolase	+
D-Mannitol	+	α-Galactosidase	–
N-acetyl-glucosamine	+	β-Galactosidase	–
D-Maltose	–	β-Glucuronidase	–
Gluconate	+	α-Glucosidase	–
Caprate	+	β-Glucosidase	–
Adipate	–	*N*-Acetyl-β-glucosaminidase	–
Malate	+	α-Mannosidase	–
Citrate	+	α-Fucosidase	–
Phenyl-acetate	–		

+, Positive; –, Negative; w, weakly positive.

suggest that nanoparticles are usually formed following this way: metal ions are first trapped on the surface or inside of the microbial cells. The trapped metal ions are then reduced to nanoparticles in the presence of enzymes [21]. Among the two methods, extracellular synthesis is more convenient and facile in comparison with intracellular synthesis as the synthesized nanoparticles can be easily purified. However, in case of intracellular synthesis firstly the cells should be completely harvested by centrifugation and subjected to several cycles ultra-sonication to disrupt the cells, which makes the purification step complicated. That is why in the present study we focused on extracellular synthesis.

3.3. Characterization of AgNPs

3.3.1. UV–vis

The reduction of pure Ag^+ ions to Ag^0 was monitored by measuring UV–vis spectrum of the reaction mixture. In the UV–vis absorption spectrum, the surface plasmon resonance (SPR) of silver occurred at 412 nm, which was attributed to the SPR band of AgNPs (Fig. 2A). It is known that an absorption band at about 400–420 nm is due to SPR in nano-silver. SPR bands appearing in the visible region are characteristics of the noble metal nanoparticles [22].

3.3.2. FE-TEM

FE-TEM results revealed the irregular shape of synthesized AgNPs with size range from 10 to 40 nm (Figs. 2B and C). Previously, we reported the roughly spherical shape of AgNPs synthesized form *Aeromonas* THG-FG1.2 and *Kinneretia* THG-SQI4 [23,24]. Analysis through EDX spectrometer confirmed the presence of elemental signal of the silver and homogenous distribution of AgNPs (Fig. 3A). The EDX spectrum of AgNPs generally showed typical absorption peak approximately at 3 keV [15]. The appearance of peak for copper (Cu) corresponds to the TEM grid used for the study. The elemental mapping results of the nanoparticles indicate the maximum distribution of silver elements (Figs. 3B and C).

3.3.3. XRD

The XRD pattern of the AgNPs revealed some diffraction peaks

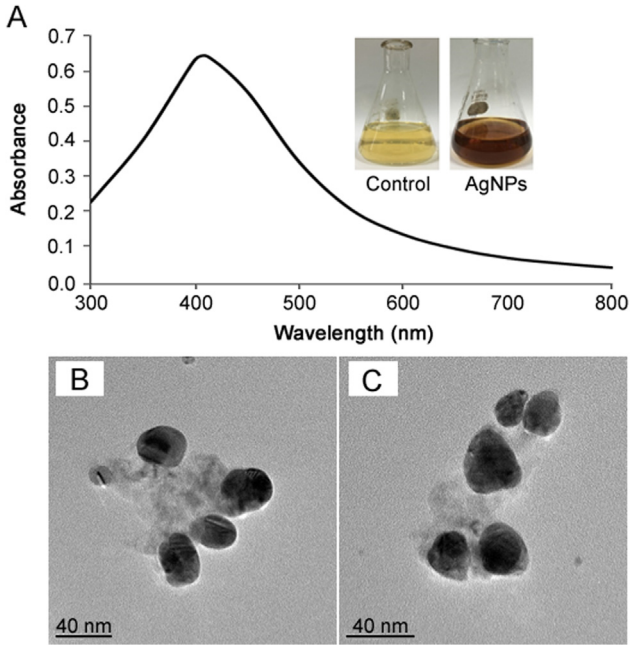

Fig. 2. UV–vis spectra of reaction mixture (A). FE-TEM image of silver nanoparticles (B and C).

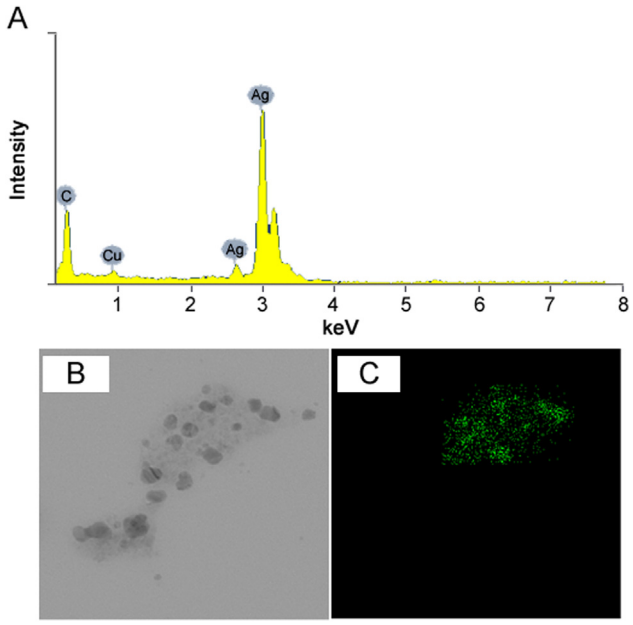

Fig. 3. EDX and elemental mapping results of (AgNPs). AgNPs observed in EDX spectrum (A), electron micrograph region (B), and distribution of silver in elemental mapping (C).

at 2θ of about 38.116°, 44.227°, 64.426°, 77.472° and 81.536° which were indexed to the 111, 200, 220, 311 and 222 orientations, respectively. All these diffraction peaks were matched to the face centered cubic (fcc) phase of Ag^0 standard (JCPDS Card no. 04-0783). These sharp Bragg peaks might have resulted from the capping agent stabilizing the nanoparticle. Intense Bragg reflections suggest that strong X-ray scattering centers in the crystalline phase and could be due to capping agents. The XRD result is in line with that of the recently reported work [10,24,25]. The absence of other peaks signifies the purity of synthesized AgNPs. The sharp ring pattern in SAED further reveals the crystalline structure of the AgNPs (Fig. 4). The rings in SAED pattern correspond to the following reflections at 111, 200, 220, 311 and 222. The XRD and

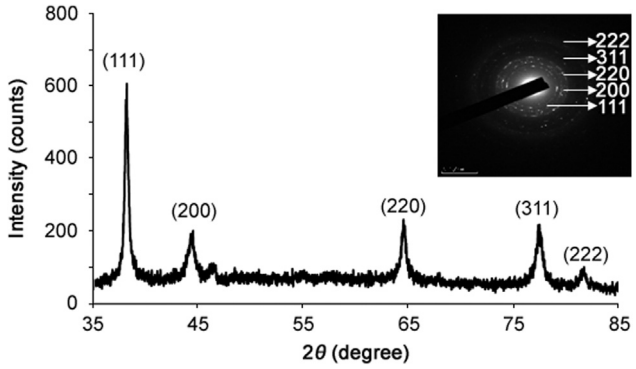

Fig. 4. X-ray diffraction pattern of synthesized silver nanoparticles. Inset showing SAED pattern.

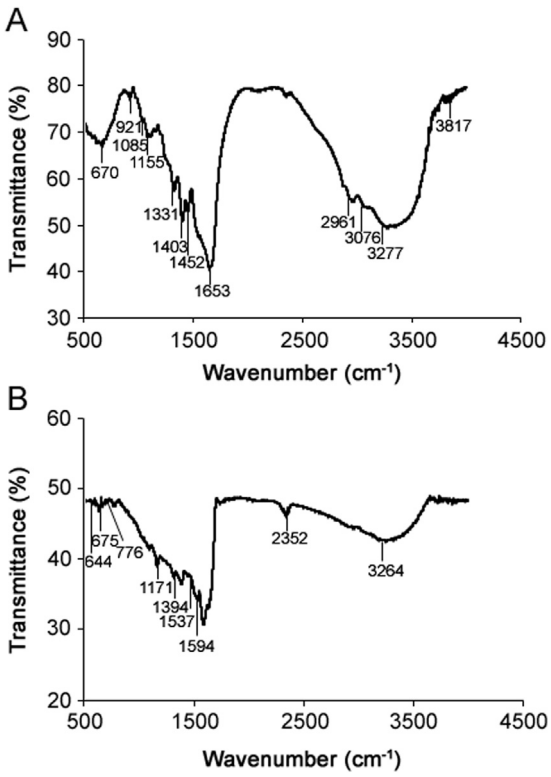

Fig. 5. FT-IR spectra of bacterial supernatant (A) and synthesized silver nanoparticles (B).

SAED pattern confirms the crystalline structure of synthesized AgNPs.

3.3.4. FT-IR

Fig. 5 shows the FT-IR spectrum recorded from the freeze-dried powder of bacterial supernatant and AgNPs. The amide linkages between amino acid residues in proteins give rise to the well-known signatures in the infrared region of the electromagnetic spectrum. The bands seen at 3277, 3076, 2961, 2352, 1331 and 1394 cm^{-1} were assigned to the stretching vibrations of alcohol (O–H), primary amines (N–H), alkane (C–H), amine (C–N), and alcohol (C–O) groups, respectively. Amide bands containing carbonyl groups (C═O) were observed at 1653 and 1594 cm^{-1}. The bands observed at 1452, 1403, 1155 and 1171 cm^{-1} can be assigned to the C–O stretching vibrations of aromatic and aliphatic amines, respectively. This result suggests that the biological molecules could possibly perform a function for the formation and stabilization of AgNPs in an aqueous medium. The overall observation

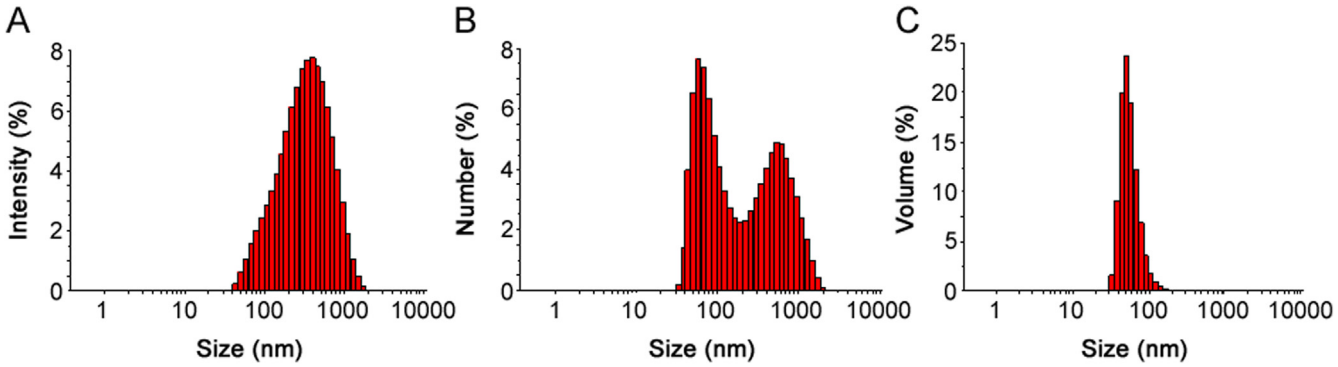

Fig. 6. Particle size distribution of silver nanoparticles (AgNPs), with respect to intensity (A), number (B) and volume (C). The average size (± SD) of AgNPs was analyzed in triplicate and typical results has been shown in the figure.

confirms the presence of protein in AgNPs. It was reported earlier that proteins can bind to nanoparticles through either free amine groups or cysteine residues in the proteins [26] and, therefore, provide stabilization of the AgNPs.

3.3.5. DLS

The average size of AgNPs was determined using DLS. Fig. 6 shows the particle size distribution of AgNPs based on intensity, volume and number. The average size of AgNPs analyzed shows the "Z" range average values of about 228.7 ± 2.4 nm with polydisperse value (0.369). The polydispersity value signifies the good quality of synthesized AgNPs. Recently, reported work has shown the average size of synthesized AgNPs from bacteria wes 50–150 nm, 110 nm, and 102 nm [5,8,10].

3.4. Antimicrobial activity of AgNPs

The antibiotic resistance mechanism in microorganisms has become a major concern and has received considerable attention in the medical field [16]. The AgNPs have been well demonstrated for their antimicrobial efficacy [13,24,25,27]. In the present study, the biosynthesized AgNPs have been tested for their antimicrobial efficacy against clinical pathogens. Results show that AgNPs have a significant antimicrobial activity against various pathogenic strains such as *B. cereus*, *S. aureus*, *C. tropicalis, V. parahaemolyticus*, *E. coli*, *P. aeruginosa* and *S. enterica* (Fig. 7). The average zone of inhibition results is shown in Table 2. It was evident from the observations that the biosynthesized AgNPs were able to restrict the pathogenic strains and may have potential to be used in medical field. Several mechanisms have been reported for the antimicrobial activity of AgNPs but the exact mechanism has not been established yet. Most widely accepted mechanism is that positively charged silver ions can interact with negatively charged phosphorus or sulfur containing biomacromolecular compounds (proteins and nucleic acid), causing structural changes and deformation of bacterial cell wall and membrane that leads to disruption of metabolic process and followed by cell death [28]. Reports also suggest that membrane damage is due to free radical derived from the surface of nanoparticles, causing a significant increase in membrane permeability and leading to cell death [29].

In recent years, AgNPs has been tested for tremendous applications like on protective clothing [30], and on patients for trauma and dental implants, prostheses and bone cement [31]. Several studies have reported the synergistic effect of AgNPs with antibiotics microorganisms [5,32,33]. As a result, the biosynthesized AgNPs were also tested for enhancing the antibacterial activity of commercial antibiotics against pathogenic bacteria including *P. aeruginosa, E. coli* and *S. enterica.* All the three clinical

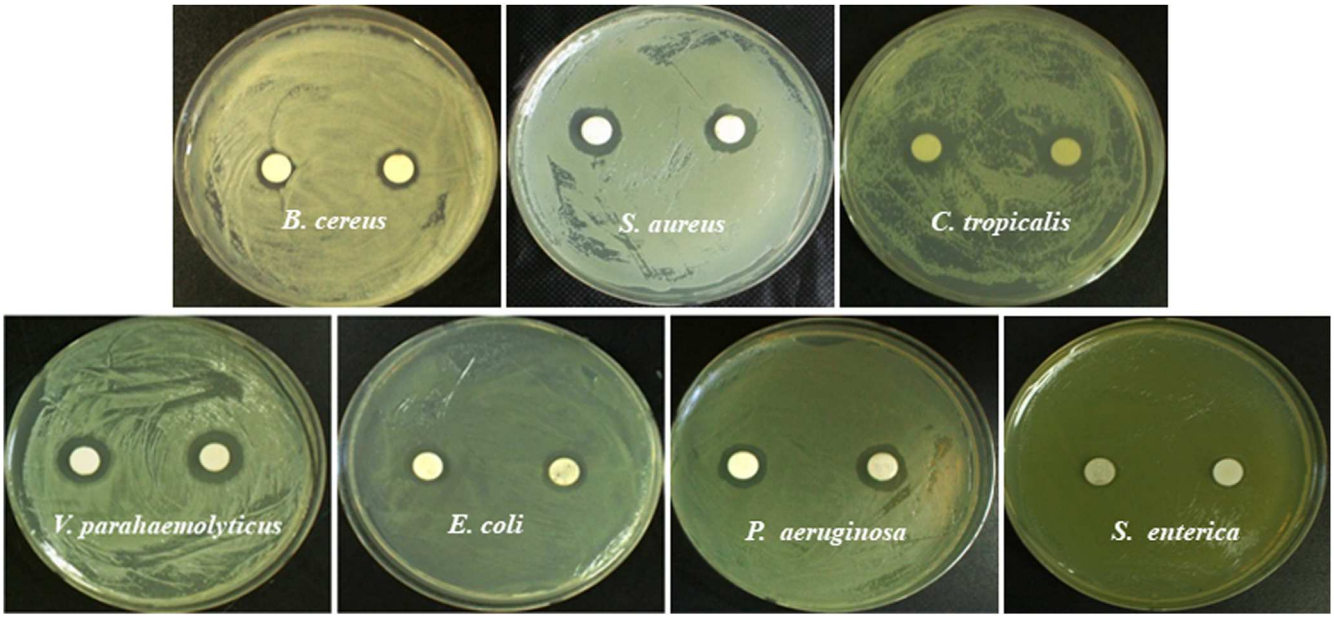

Fig. 7. Zones of inhibition of 30 μL of silver nanoparticle (in water) against *Bacillus cereus, Staphylococcus aureus, Candida tropicalis, Vibrio parahaemolyticus, Escherichia coli, Pseudomonas aeruginosa and Salmonella enterica.*

Table 2
Antimicrobial activity of the AgNPs synthesized from *Psuedomonas koreensis* THG-LS1.4.

Pathogenic species	Zone of inhibition ± SD
Candida tropicalis [KCTC 17762]	16.5 ± 0.6
Bacillus cereus [KACC 11240]	11.5 ± 0.7
Staphylococcus aureus [KCTC 3881]	16.0 ± 0.2
Pseudomonas aeruginosa [KACC 14021]	14.5 ± 0.5
Escherichia coli [CCARM 0237]	13.0 ± 0.3
Vibrio parahaemolyticus [KACC 15069]	16.5 ± 0.5
Salmonella enterica [KACC 10763]	11.5 ± 0.8

bacterial isolates were resistant to the commercial antibiotics erythromycin, novobiocin, lincomycin, penicillin G, vancomycin and oleandomycin (Figs. 8A-F). The results found that when the AgNPs were added over the antibiotic discs the sensitivity of bacteria increased and resulted in the formation of zone of inhibition (Figs. 8G-L). The results were interpreted in terms of standard deviation of mean diameter of zone of inhibition (Table 3). The average increase in sensitivity pattern of antibiotics was calculated by average increase in fold area [8]. The average increase in fold area of the antibiotics against antibiotics resistant bacteria was the greatest for erythromycin, followed by novobiocin, penicillin G, oleandomycin, lincomycin and then vancomycin. Studies suggested that the increase in synergistic effect may be caused by the bonding reaction between antibiotic and nanosilver. The antibiotic molecules contain many active groups such as hydroxyl and amido groups, which react easily with nanosilver by chelation [32]. Results are consistent with those of earlier studies where the AgNPs

Table 3
Individual and combined efficacy of commercial antibiotics and biosynthesized AgNPs against pathogenic bacteria.

Pathogenic Bacteria	Antibiotic	Inhibition Zone	
		Ab	Ab + AgNPs
P. aeruginosa	Erythromycin	-	15.0 ± 1.1
	Novobiocin	-	15.0± 0.8
	Vancomycin	-	13.0± 2.1
	Lincomycin	-	14.0± 1.5
	Penicillin G	-	14.0± 1.3
	Oleandomycin	-	14.0± 1.5
E. coli	Erythromycin	-	13.0± 2.2
	Novobiocin	-	11.0± 1.8
	Vancomycin	-	11.0± 1.8
	Lincomycin	-	11.0± 1.7
	Penicillin G	-	12.0± 1.1
	Oleandomycin	-	11.0 ± 2.0
S. enterica	Erythromycin	-	13.0± 1.9
	Novobiocin	-	13.0± 1.6
	Vancomycin	-	11.0 ± 2.3
	Lincomycin	-	11.0 ± 1.9
	Penicillin G	-	10.0 ± 2.1
	Oleandomycin	-	11.0± 2.5

Notes: Ab: Antibiotic.
Ab + AgNPs: Antibiotics with silver nanoparticles.
Erythromycin (15 μg/disc), Lincomycin (15 μg/disc), Novobiocin (30 μg/disc), Penicillin G (10 μg/disc), Vancomycin (30 μg/disc) and Oleandomycin (15 μg/disc). AgNPs: silver nanoparticles, 30 μL (500 ppm). Each result is a representative of three independent experiment. Results are expressed as means ± standard deviation (SD).

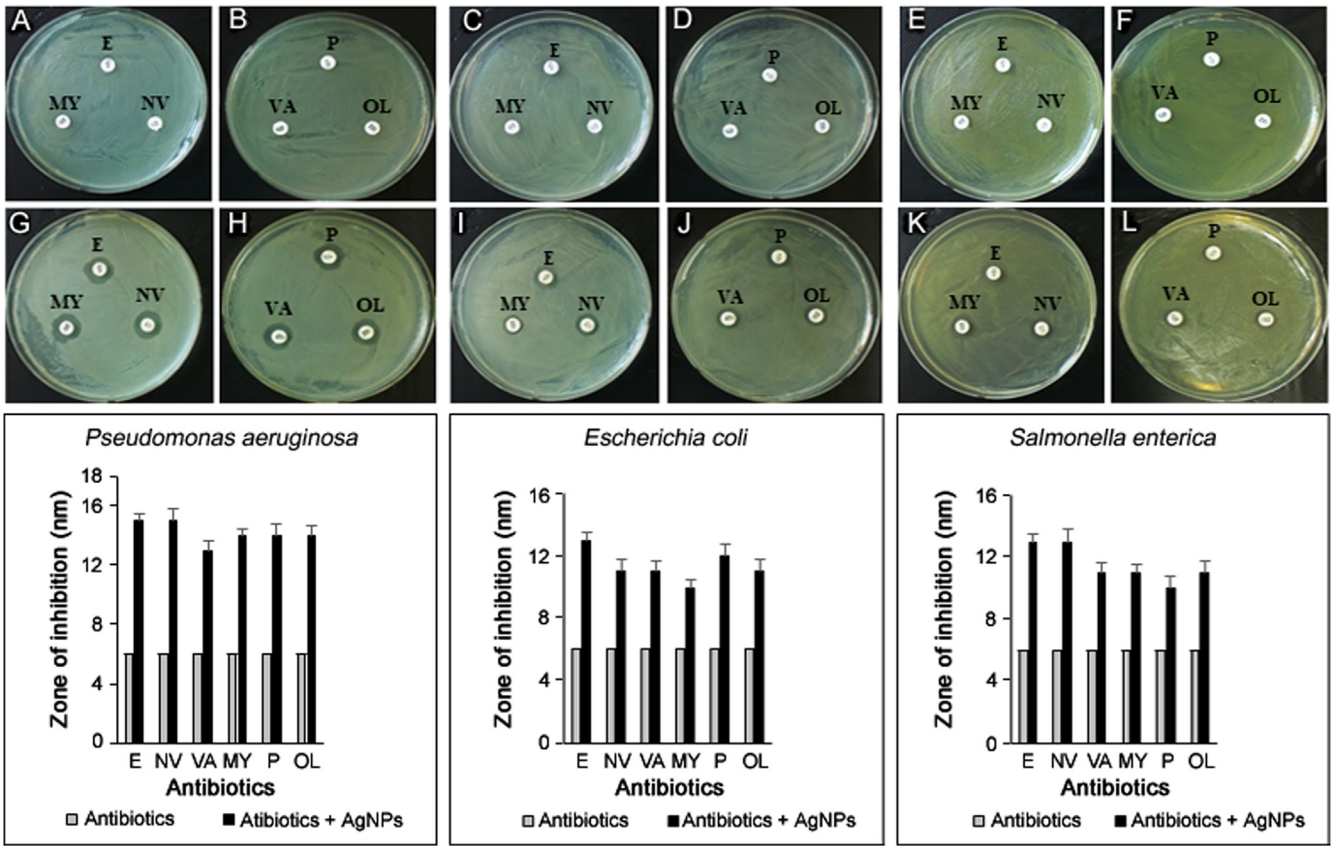

Fig. 8. Zones of inhibition of standard antibiotic dics against *Pseudomonas aeruginosa* (A and B), *Escherichia coli* (C and D), *Salmonella enterica* (E and F). Zone of inhibition of standard antibiotic dics with silver nanoparticles against *Pseudomonas aeruginosa* (G and H), *Escherichia coli* (I and J), *Salmonella enterica* (K and L). Note: (E) Erythromycin 15 μg/disc, (MY) Lincomycin 15 μg/disc, (NV) Novobiocin 30 μg/disc, (P) Penicillin G 10 μg/disc, (VA) Vancomycin 30 μg/disc and (OL) Oleandomycin 15 μg/disc; AgNPs: silver nanoparticles, 30 μL (500 ppm).

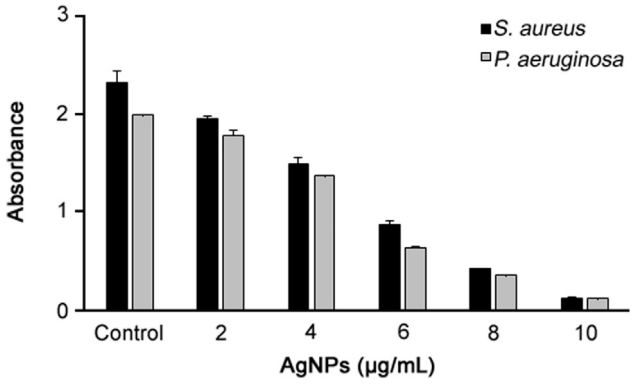

Fig. 9. Biofilm inhibition activity of silver nanoparticles against *S. aureus* and *P. aeruginosa*.

demonstrated enhanced antibacterial activity with antibiotics against pathogenic microorganisms [8,32,33]. Moreover, the AgNPs were shown to enhance the effect of commercial antibiotics against resistant bacteria. Additionally, the results of the biofilm inhibition were found positive, and the results showed that the AgNPs could inhibit the biofilm at a concentration of 10 µg/mL against *S. aureus* and *P. aeruginosa*. (Fig. 9). Our results were consistent with those of previously reported work by Kalishwaralal et al. [34].

4. Conclusion

The present study demonstrated the eco-friendly, facile and extracellular synthesis of AgNPs through *Pseudomonas* sp. THG-LS1.4. These biosynthesized AgNPs were further confirmed by using UV–vis spectroscopy, FE-TEM and XRD analysis. The AgNPs have antimicrobial efficacy and are capable of enhancing the antibacterial effect of commercial antibiotics. Furthermore, AgNPs also show biofilm inhibition activity. We believe that in the future biosynthesized AgNPs have the possibility to be used for disinfection application or as a coating agent for surgical devices, instruments and wound healing bandages. However, further experiments especially in-vivo trials need to be done to confirm this.

Conflicts of interest

The authors declare that there are no conflicts of interest.

Acknowledgments

This work was conducted under the industrial infrastructure program (No. N0000888) for fundamental technologies which is funded by the Ministry of Trade, Industry and Energy (MOTIE, Korea).

References

[1] M.A. Albrecht, C.W. Evans, C.L. Raston, Green chemistry and the health implications of nanoparticles, Green Chem. 8 (2006) 417–432.
[2] P.S. Schabes-Retchkiman, G. Canizal, R. Herrera-Becerra, et al., Biosynthesis and characterization of Ti/Ni bimetallic nanoparticles, Opt. Mater. 29 (2006) 95–99.
[3] H. Gu, P.L. Ho, E. Tong, et al., Presenting vancomycin on nanoparticles to enhance antimicrobial activities, Nano. Lett. 3 (2003) 1261–1263.
[4] Z. Ahmad, R. Pandey, S. Sharma, et al., Alginate nanoparticles as antituberculosis drug carriers: formulation development, pharmacokinetics and therapeutic potential, Ind. J. Chest Dis. Allied Sci. 48 (2006) 171–176.
[5] P. Singh, Y.J. Kim, H. Singh, et al., Biosynthesis, characterization, and antimicrobial applications of silver nanoparticles, Int. J. Nanomed. 10 (2015) 2567–2577.
[6] A. Majdalawieh, M.C. Kanan, O. El-Kadri, et al., Recent advances in gold and silver nanoparticles: synthesis and applications, J. Nanosci. Nanotechnol. 14 (2014) 4757–4780.
[7] P. Gong, H. Li, X. He, K. Wang, et al., Preparation and antibacterial activity of Fe_3O_4@ Ag nanoparticles, Nanotechnology 18 (2007) 604–611.
[8] P. Singh, Y.J. Kim, H. Singh, et al., Biosynthesis of anisotropic silver nanoparticles by *Bhargavaea indica* and their synergistic effect with antibiotics against pathogenic microorganisms, J. Nanomater. 2015 (2015) 4–14.
[9] P. Singh, Y.J. Kim, D. Zhang, et al., Biological synthesis of nanoparticles from plants and microorganisms, Trends Biotechnol. 34 (2016) 588–599.
[10] P. Singh, H. Singh, Y.J. Kim, et al., Extracellular synthesis of silver and gold nanoparticles by *Sporosarcina koreensis* DC4 and their biological applications, Enzym. Microb. Technol. 86 (2016) 75–83.
[11] S. Rajeshkumar, C. Malarkodi, K. Paulkumar, et al., Intracellular and extracellular biosynthesis of silver nanoparticles by using marine bacteria *Vibrio alginolyticus*, J. Nanosci. Nanotechnol. 3 (2013) 21–25.
[12] D. Mandal, M.E. Bolander, D. Mukhopadhyay, et al., The use of microorganisms for the formation of metal nanoparticles and their application, Appl. Microbiol. Biotechnol. 69 (2006) 485–492.
[13] P. Velusamy, G.V. Kumar, V. Jeyanthi, et al., Bio-inspired green nanoparticles: synthesis, mechanism, and antibacterial application, Toxicol. Res. 32 (2016) 95–102.
[14] J.H. Jo, P. Singh, Y.J. Kim, et al., *Pseudomonas deceptionensis* DC5-mediated synthesis of extracellular silver nanoparticles, Artif. Cells Nanomed. Biotechnol. 44 (2016) 1576–1581.
[15] C. Wang, Y.J. Kim, P. Singh, et al., Green synthesis of silver nanoparticles by *Bacillus methylotrophicus*, and their antimicrobial activity, Artif. Cells Nanomed. Biotechnol. 44 (2016) 1127–1132.
[16] S.A. Kumar, M.K. Abyaneh, S.W. Gosavi, et al., Nitrate reductase-mediated synthesis of silver nanoparticles from $AgNO_3$, Biotechnol. Lett. 29 (2007) 439–445.
[17] S.A. Kumar, M.K. Abyaneh, S.W. Gosavi, et al., Sulfite reductase-mediated synthesis of gold nanoparticles capped with phytochelatin, Biotechnol. Appl. Biochem. 47 (2007) 191–195.
[18] O.S. Kim, Y.J. Cho, K. Lee, et al., Introducing EzTaxon-e: a prokaryotic 16S rRNA gene sequence database with phylotypes that represent uncultured species, Int. J. Syst. Evol. Microbiol. 62 (2012) 716–721.
[19] N. Saitou, M. Nei, The neighbor-joining method: a new method for reconstructing phylogenetic trees, Mol. Biol. Evol. 4 (1987) 406–425.
[20] K. Tamura, G. Stecher, D. Peterson, et al., MEGA6: molecular evolutionary genetics analysis version 6.0, Mol. Biol. Evol. 30 (2013) 2725–2729.
[21] O.V. Singh, Bio-nanoparticles: Biosynthesis and Sustainable Biotechnological Implications, John Wiley & Sons, New York, 2015.
[22] N. Singh, P.K. Khanna, In situ synthesis of silver nano-particles in polymethylmethacrylate, Mater. Chem. Phys. 104 (2007) 367–372.
[23] H. Singh, J. Du, T.H. Yi, Biosynthesis of silver nanoparticles using *Aeromonas* sp. THG-FG1.2 and its antibacterial activity against pathogenic microbes, Artif. Cells Nanomed. Biotechnol. 45 (2017) 584–590.
[24] H. Singh, J. Du, T.H. Yi, *Kinneretia* THG-SQI4 mediated biosynthesis of silver nanoparticles and its antimicrobial efficacy, Artif. Cells Nanomed. Biotechnol. 45 (2017) 602–608.
[25] J. Du, T.H. Yi, Biosynthesis of silver nanoparticles by *Variovorax guangxiensis* THG-SQL3 and their antimicrobial potential, Mater. Lett. 178 (2016) 75–78.
[26] A. Gole A, C. Dash, V. Ramachandran, et al., Pepsin-gold colloid conjugates: preparation, characterization, and enzymatic activity, Langmuir 17 (2001) 1674–1679.
[27] M.K. Rai, S.D. Deshmukh, A.P. Ingle, et al., Silver nanoparticles: the powerful nanoweapon against multidrug-resistant bacteria, J. Appl. Microbiol. 112 (2012) 841–852.
[28] S. Shankar, J.W. Rhim, Amino acid mediated synthesis of silver nanoparticles and preparation of antimicrobial agar/silver nanoparticles composite films, Carbohydr. Polym. 130 (2015) 353–363.
[29] J.S. Kim, E. Kuk, K.N. Yu, et al., Antimicrobial effects of silver nanoparticles, Nanomed. Nanotechnol. Biol. Med. 3 (2007) 95–101.
[30] N. Farhadian, R.U. Mashoof, S. Khanizadeh, et al., *Streptococcus mutans* counts in patients wearing removable retainers with silver nanoparticles vs those wearing conventional retainers: a randomized clinical trial, Am. J. Orthod. Dentofac. Orthop. 149 (2016) 155–160.
[31] H. Zazo, C.I. Colino, J.M. Lanao, Current applications of nanoparticles in infectious diseases, J. Control. Release 224 (2016) 86–102.
[32] A.M. Fayaz, K. Balaji, M. Girilal, et al., Biogenic synthesis of silver nanoparticles and their synergistic effect with antibiotics: a study against gram-positive and gram-negative bacteria, Nanomed. Nanotechnol. Biol. Med. 6 (2010) 103–109.
[33] S.Z. Naqvi, U. Kiran, M.I. Ali, et al., Combined efficacy of biologically synthesized silver nanoparticles and different antibiotics against multidrug-resistant bacteria, Int. J. Nanomed. 8 (2013) 3187–3195.
[34] K. Kalishwaralal, S. BarathManiKanth, S.R. Pandian, et al., Silver nanoparticles impede the biofilm formation by *Pseudomonas aeruginosa* and *Staphylococcus epidermidis*, Colloids Surf. B Biointerfaces 79 (2010) 340–344.